Available online at www.sciencedirect.com
ScienceDirect
J. Mater. Sci. Technol., 2011, **27**(11), 1001-1005.
JMST
www.JMST.org

In-situ One-pot Preparation of $LiFePO_4$/Carbon-Nanofibers Composites and Their Electrochemical Performance

Jiaohui Zhang, Jian Xie, Chunyang Wu, Gaoshao Cao and Xinbing Zhao†
Department of Materials Science and Engineering, Zhejiang University, Hangzhou 310027, China
[Manuscript received July 22, 2011, in revised form August 22, 2011]

A novel *in-situ* route was employed to synthesize $LiFePO_4$/carbon-nanofibers (CNFs) composites. The route combined high-temperature solid phase reaction with chemical vapor deposition (CVD) using Fe_2O_3 and LiH_2PO_4 as the precursors for $LiFePO_4$ growth and acetylene (C_2H_2) as the carbon source for CNFs growth. The composites were characterized by X-ray diffraction (XRD), Brunauer-Emmett-Teller (BET) specific surface area, field emission scanning electron microscopy (FE-SEM), and transmission electron microscopy (TEM). The electrochemical performance of the composites was studied by galvanostatic cycling and cyclic voltammetry (CV). The results showed that the *in-situ* CNFs growth could be realized by the catalytic effect of the Fe_2O_3 precursor. The sample after 80 min CVD reaction showed the best electrochemical performance, indicating a promising application in high-power Li-ion batteries.

KEY WORDS: $LiFePO_4$/carbon-nanofibers; *In-situ* catalytic growth; 3D conductive network; Electrochemical performance

1. Introduction

Since first reported by Padhi *et al.*[1,2], olivine-type lithium iron phosphate, $LiFePO_4$, has attracted an increasing interest as a promising cathode material for large size Li-ion batteries for electric vehicles (EVs) and hybrid electric vehicles (HEVs). The main shortcomings of this material are its intrinsically poor electrical conductivity and low Li-ion diffusion rate. To date, the most effective method to increase the electronic conductivity of $LiFePO_4$ is carbon coating[3]. In recent years, various forms of carbon materials have been proposed to coat $LiFePO_4$, such as carbon black[4–8], graphite[6–9] and pyrolytic carbon[3,10–12].

Recently, the one-dimensional (1D) carbon materials: carbon nanotubes (CNTs)[13–21] and carbon nanofibers (CNFs)[6,22], have also been used to enhance the electronic conductivity of $LiFePO_4$. In the above work, CNTs or CNFs were incorporated into $LiFePO_4$ through an *ex-situ* route, namely that, the CNTs or CNFs was prepared in advance. In this work, CNFs was introduced into $LiFePO_4$ through a novel *in-situ* route. In other words, the growth of $LiFePO_4$ and CNFs can occur simultaneously. The microstructure and electrochemical performance of the *in-situ* prepared $LiFePO_4$/CNFs were investigated.

2. Experimental

The $LiFePO_4$/CNFs composites were prepared by solid phase reaction combined with chemical vapor deposition (CVD). The precursors were sufficiently mixed by ball-milling stoichiometric LiH_2PO_4 (analytical reagent) and Fe_2O_3 (analytical reagent) in acetone for 10 h at 300 r/min with a ball-to-precursors weight ratio of 9:1 followed by drying at 60°C for 8 h in air. The procedure for the solid phase reaction was as follows: first, the precursors mixture was heated in flowing N_2 from room temperature to 500°C; second, the temperature was maintained at 500°C for a period of time (60, 80, 100 and 120 min) in flowing N_2/C_2H_2 (10 vol.% C_2H_2); third, the temperature was then increased to 700°C and the gas was switched to

† Corresponding author. Prof., Ph.D.; Tel.: +86 571 87951451; Fax: +86 571 87951451; E-mail address: zhaoxb@zju.edu.cn (X.B. Zhao).

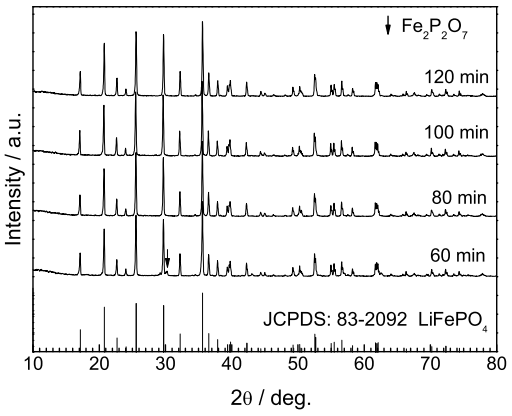

Fig. 1 XRD patterns of the products with different period of CVD reaction time

N_2; finally, the heating was continued for 5 h in N_2 followed by cooling to room temperature naturally.

The crystalline structure of the obtained products was characterized by X-ray diffraction (XRD) on a Rigaku D/Max-2550pc powder diffractometer equipped with Cu$K\alpha$ radiation (λ=0.1541 nm). The morphology of the products was observed by field emission scanning electron microscopy (FE-SEM) on an FEI-sirion microscope and transmission electron microscopy (TEM) on a JEM-2110. The carbon content was measured on a Flash EA 1112 tester. The specific surface area of the samples was measured by using the Brunauer-Emmett-Teller (BET) method under an AUTOSORB-1-C instrument.

$LiFePO_4$/CNFs, acetylene black and polyvinylidene fluoride (PVDF) binder in a weight ratio of 80:10:10 were mixed in N-methyl pyrrolidone (NMP) and stirred for 2 h to make slurry. The working electrodes were prepared by spreading the slurry on Al foils and dried at 60°C for 8 h in air. The CR2025-type coin cells were assembled in an Ar-filled glove box using metallic lithium as anode, 1 mol/L $LiPF_6$ solution in ethylene carbonate (EC)/dimethyl carbonate (DMC) (1:1 in volume) as electrolyte, and Celgard 2300 porous polypropylene film as separator. Galvanostatic cycling was performed between 2.5 and 4.3 V *vs* Li/Li^+ at various C rates on a PCBT-138-32D battery tester, where 1 C corresponds to 170 $mA{\cdot}g^{-1}$. Cyclic voltammetry (CV) was performed between 2.5 and 4.3 V at 0.1 $mV{\cdot}s^{-1}$ using a CHI660C electrochemical workstation. All of the electrochemical measurements were performed at 25°C.

3. Results and Discussion

Figure 1 shows the XRD patterns of the products prepared by solid phase reaction combined with CVD treatment. For comparison, the standard diffraction patterns of $LiFePO_4$ are also presented. For sample after 60 min CVD treatment, a small $Fe_2P_2O_7$ peak is detected. All the XRD patterns of the other samples can be indexed to single-phased olivine-type $LiFePO_4$ with a space group *Pmnb*. No diffraction peaks related to carbon can be found, indicating that it is not well crystallized or at a low content. The formation of $LiFePO_4$ can be written as

$$Fe_2O_3+2LiH_2PO_4+C \rightarrow 2LiFePO_4+CO+2H_2O \quad (1)$$

where Fe_2O_3 and LiH_2PO_4 are used as the precursors in the presence of carbon. The carbon comes from the pyrolysis of C_2H_2 in this work:

$$C_2H_2 \rightarrow 2C + H_2 \quad (2)$$

The carbon contents of the samples after 80, 100 and 120 min CVD reaction are 3.5, 5.6, and 7.1 wt%, respectively. Note that a reasonable carbon content of 3.5 wt% was achieved after 80 min CVD reaction, and that increasing the CVD reaction time will deposit more carbon. For the calculation of the gravimetric capacity, the weight of carbon is included for all the samples. The specific surface area by the BET method is 5.2 $m^2{\cdot}g^{-1}$ for the sample after 80 min CVD reaction. For comparison, another $LiFePO_4$/C sample was synthesized using Fe_2O_3 and LiH_2PO_4 as the precursors and polypropylene as the carbon source. This sample shows a lower specific surface area of 3.8 $m^2{\cdot}g^{-1}$, even though the two samples have the same carbon content of 3.5%. It is also found that the slurry made of $LiFePO_4$/CNFs is easier to coat than that made of $LiFePO_4$/C.

Figure 2 shows the SEM images of samples after different period of the CVD time. Note that the sample after 80 min CVD reaction is composed of microsized particles and fiber-like 1D material as shown in Fig. 2(a). It seems that the particles are connected by the 1D material with its end embedded into the particles. The amount of the 1D material is obviously increased when the CVD reaction time is increased to 100 min as seen in Fig. 2(b). After 120 min CVD reaction, some thick 1D material appears in addition to the thin ones (Fig. 2(c)), which is responsible for the remarkable increase in the carbon content. According to the XRD results and the carbon content analyses, the microsized particles are considered to be $LiFePO_4$, while the fiber-like 1D material is CNFs. As a result, a three-dimensional (3D) conductive network for $LiFePO_4$ particles has been formed by the inter-entangled CNFs. It is expected that the CNFs can maintain a firm contact with the $LiFePO_4$ particles due to the *in-situ* route.

The microstructure of the 80 min CVD sample was further characterized by TEM as shown in Fig. 3. It is clear that the $LiFePO_4$ particles are entangled by the CNFs (Fig. 3(a)) to construct the 3D electronically conductive network. A good electronic conductivity, therefore, can be anticipated for the $LiFePO_4$/CNFs

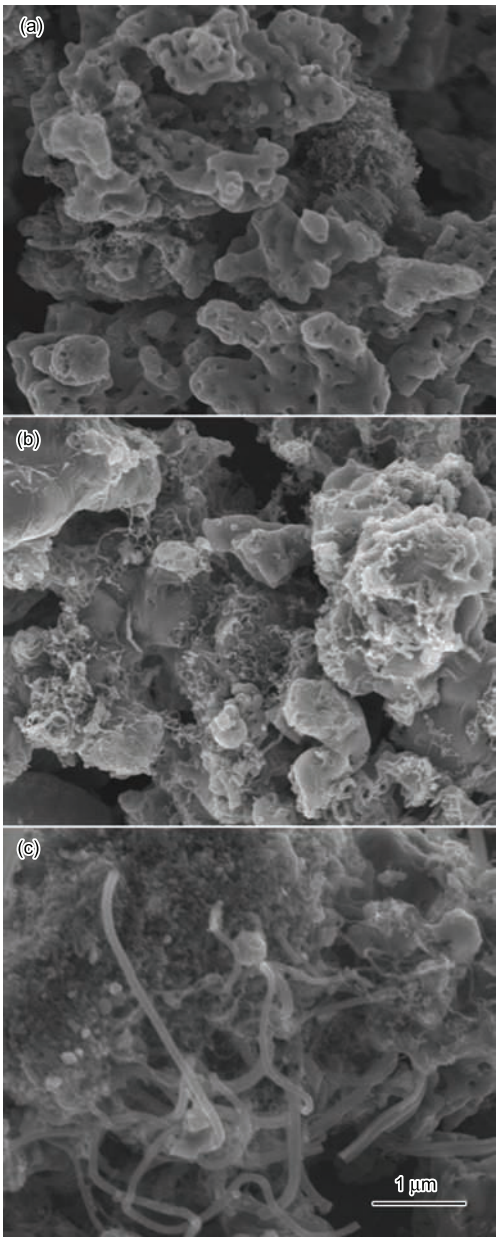

Fig. 2 SEM images of the products after 80 (a), 100 (b), and 120 min (c) CVD reaction

composite, which is critical for the high-power application. Figure 3(b) shows the TEM image of a $LiFePO_4$ particle with attached CNFs. Obviously, the ends of the CNFs are embedded into the $LiFePO_4$ particle. The diameter of the CNFs is in the range of 20–30 nm. The growth of the CNFs is considered to be catalyzed by Fe_2O_3. In the separate experiments, the possibility that the LiH_2PO_4 or $LiFePO_4$ can catalytically grow CNFs, can be excluded.

The charge (Li-extraction) and discharge (Li-reinsertion) curves at various rates are presented in Fig. 4. In these tests, the gravimetric capacity is based on the total weight of $LiFePO_4$ and CNFs. All of the samples exhibit flat charge (3.46 V) and discharge (3.41 V) plateaus, indicative of a good crystallization of $LiFePO_4$ at 0.1 C.

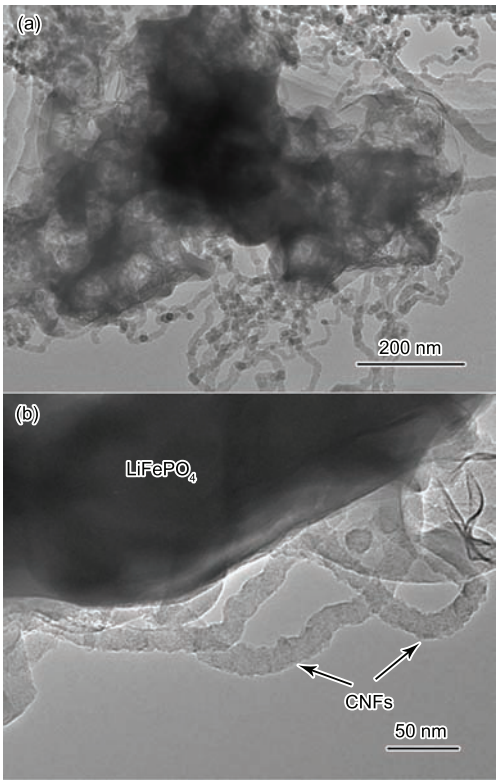

Fig. 3 TEM images of the products after 80 min CVD reaction

The sample after 80 min CVD reaction yields the highest discharge capacity of 153 $mAh \cdot g^{-1}$. The discharge capacity of the 80 min CVD sample is still the highest based on the weight of bare $LiFePO_4$. This suggests that only a trace amount of Fe_2O_3 takes place in the catalytic growth of CNFs, and that the growth rate of $LiFePO_4$ is rather higher than that of CNFs, in agreement with the XRD results. In contrast, the relatively low capacity for other samples suggests that a higher proportion of Fe_2O_3 was consumed during the catalytic growth of CNFs, in consistent with the carbon content analyses. At relatively high rates (1 C and 2 C), the 120 min CVD sample exhibits similar discharge capacities as the 80 min CVD sample. At a 5 C rate, however, the 80 min CVD sample shows a higher discharge capacity and a higher Coulombic efficiency than the 120 min CVD sample.

Figure 5 shows the comparison of the rate capability among the three samples. It is obvious that the 80 min CVD sample displays the best rate capability. Although all of the samples exhibit a good cycling stability at each current rate, the 80 min CVD sample shows the highest capacity. The good rate capability of this sample can be ascribed to the most efficient 3D conductive network constructed by the inter-entangled CNFs bridging and connecting the $LiFePO_4$ particles even though at a lower CNFs content. Figure 6 shows the CV plots of the 80 min CVD sample after cycling for 1 and 50 times. Note that sharp and highly symmetric redox peaks can be maintained after cycling for 50 times, indicating good electrochemical

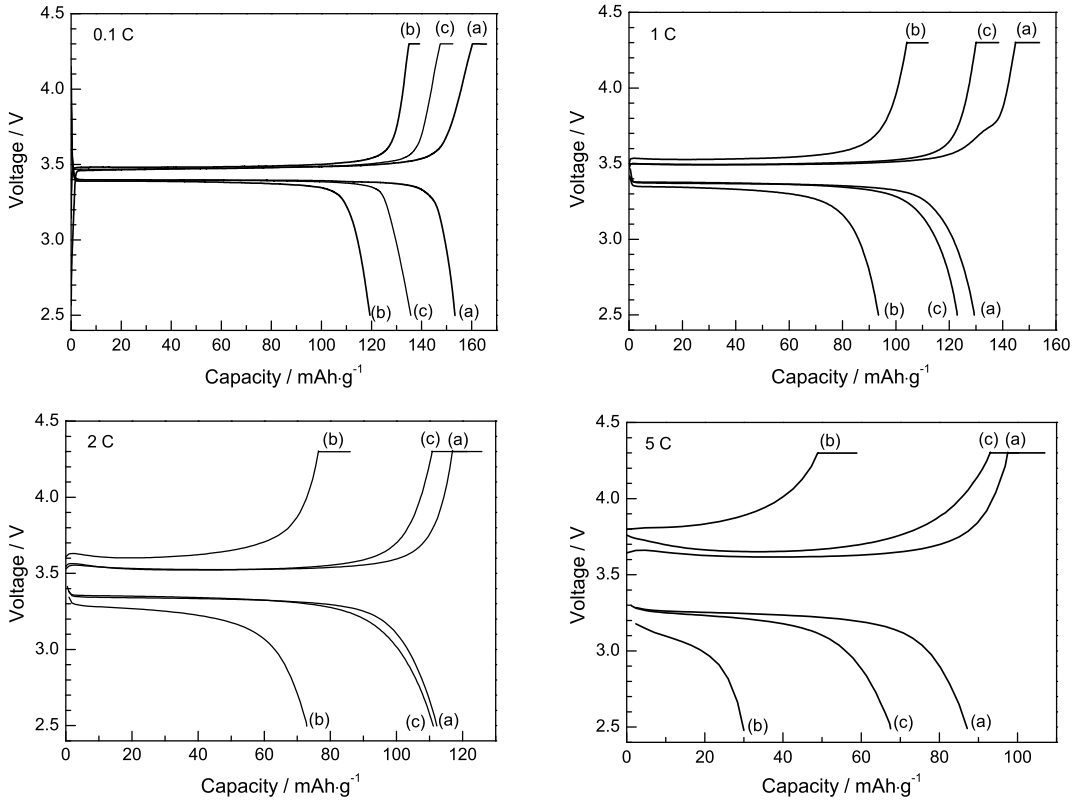

Fig. 4 Charge and discharge curves at various rates of the samples after (a) 80, (b) 100 and (c) 120 min CVD reaction

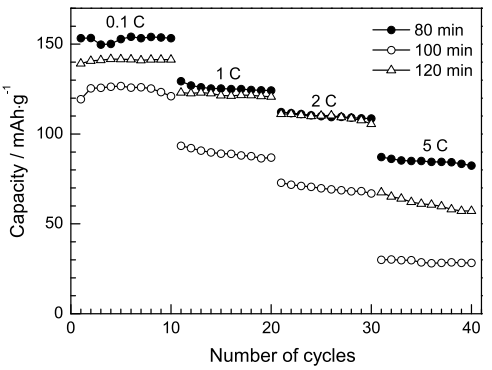

Fig. 5 Comparison of rate capability among the three samples

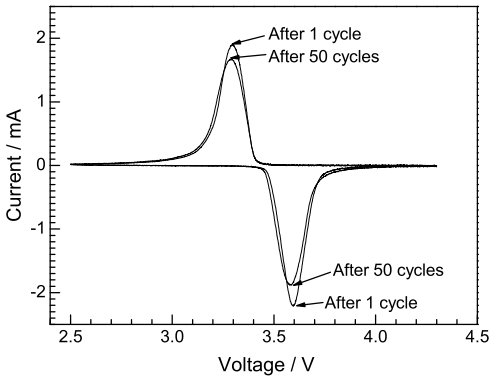

Fig. 6 CV plots of the 80 min CVD sample after cycling for 1 and 50 times

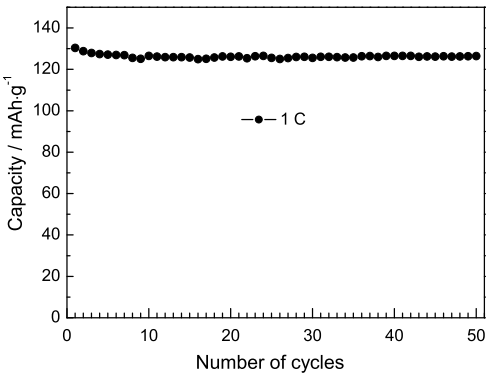

Fig. 7 Cycling stability of the 80 min CVD sample after cycling for 50 times at 1 C rate

reversibility and stability. Figure 7 shows the cycling stability of the 80 min CVD sample after cycling for 50 times at 1 C rate. After 50 cycles, the sample keeps a retention rate of 97%. The excellent cycling stability can be attributed to the good crystallization of this sample and the improvement of the electrical conductivity *via* CNFs coating. The good electrochemical performance suggests that this material will show a promising application as cathode for high-power Li-ion batteries.

4. Conclusion

In this work, $LiFePO_4$/CNFs composites were successfully synthesized by an *in-situ* route combining solid phase reaction with CVD treatment using

Fe_2O_3, LiH_2PO_4 and C_2H_2 as the precursors. The results show that the formation of $LiFePO_4$ and CNFs occurs simultaneously with a good crystallization of $LiFePO_4$ and a reasonable carbon content. The CNFs are inter-entangled forming an efficient 3D conductive network. Among the three products, the sample after 80 min CVD reaction exhibits the highest capacity and the best rate capability, which can be attributed to the efficient 3D conductive network composed of inter-entangled CNFs bridging and connecting the $LiFePO_4$ particles. The good electrochemical performance of this sample makes it a promising cathode for high-power Li-ion batteries.

Acknowledgements

This work was supported by Zijin Program of Zhejiang University, China, the Fundamental Research Funds for the Central Universities (No. 2010QNA4003), the Ph.D. Programs Foundation of Ministry of Education of China (No. 20100101120024), the Foundation of Education Office of Zhejiang Province (No. Y201016484) and the Qianjiang Talents Project of Science Technology Department of Zhejiang Province (No. 2011R10021).

REFERENCES

[1] A.K. Padhi, K.S. Nanjundaswamy, C. Masquelier, S. Okada and J.B. Goodenough: *J. Electrochem. Soc.*, 1997, **144**, 1609.
[2] A.K. Padhi, K.S. Nanjundaswamy and J.B. Goodenough: *J. Electrochem. Soc.*, 1997, **144**, 1188.
[3] N. Ravet, Y. Chouinard, J.F. Magnan, S. Besner, M. Gauthier and M. Armand: *J. Power Sources,* 2001, **97-98**, 503.
[4] R. Dominko, M. Gaberscek, J. Drofenik, M. Bele and J. Jamnik: *Electrochim. Acta*, 2003, **48**, 3709.
[5] R. Dominko, M. Gaberscek, J. Drofenik, M. Bele, S. Pejovnik and J. Jamnik: *J. Power Sources*, 2003, **119-121**, 770.
[6] I.V. Thorat, V. Mathur, J.N. Harb and D.R. Wheeler: *J. Power Sources*, 2006, **162**, 673.
[7] K. Zaghib, J. Shim, A. Guerfi, P. Charest and K.A. Striebel: *Electrochem. Solid-State Lett.*, 2005, **8**, A207.
[8] H.C. Shin, W.I. Cho and H. Jang: *Electrochim. Acta*, 2006, **52**, 1472.
[9] J. Barker, M.Y. Saidi and J.L. Swoyer: *Electrochem. Solid-State Lett.*, 2003, **6**, A53.
[10] H. Huang, S.C. Yin and L.F. Nazar: *Electrochem. Solid-State Lett.*, 2001, **4**, A170.
[11] Z.H. Chen and J.R. Dahn: *J. Electrochem. Soc.*, 2002, **149**, A1184.
[12] J.Z. Hu, J. Xie, X.B. Zhao, H.M. Yu, X. Zhou, G.S. Cao and J.P. Tu: *J. Mater. Sci. Technol.*, 2009, **25**, 405.
[13] J.J. Chen and M.S. Whittingham: *Electrochem. Commun.*, 2006, **8**, 855.
[14] X.L. Li, F.Y. Kang, X.D. Bai and W.C. Shen: *Electrochem. Commun.*, 2007, **9**, 663.
[15] L. Wang, Y.D. Huang, R.R. Jiang and D.Z. Jia: *J. Electrochem. Soc.*, 2007, **154**, A1015.
[16] B. Jin, H.B. Gu, W.X. Zhang, K.H. Park and G.P. Sun: *J. Solid State Electrochem.*, 2008, **12**, 1549.
[17] Y.J. Liu, X.H. Li, H.J. Guo, Z.X. Wang and W.J. Peng: *J. Power Sources*, 2008, **184**, 522.
[18] T. Muraliganth, A.V. Murugan and A. Manthiram: *J. Mater. Chem.*, 2008, **18**, 5661.
[19] B. Jin, E.M. Jin, K.H. Park and H.B. Gu: *Electrochem. Commun.*, 2008, **10**, 1537.
[20] J. Xu, G. Chen and X. Li: *Mater. Chem. Phys.*, 2009, **118**, 9.
[21] Y. Feng: *Mater. Chem. Phys.*, 2010, **121**, 302.
[22] M.S. Bhuvaneswari, N.N. Bramnik, D. Ensling, H. Ehrenberg and W. Jaegermann: *J. Power Sources*, 2008, **180**, 553.